Acta Cryst. (1998). D**54**, 334–341

Structure of the Complex of Bovine Pancreatic Phospholipase A_2 with a Transition-State Analogue

KANAGARAJ SEKAR,[a] AMARENDRA KUMAR,[a] XIAOHONG LIU,[b] MING-DAW TSAI,[a,b] MICHAEL H. GELB[c] AND MUTTAIYA SUNDARALINGAM[a,b]*

[a]*Biological Macromolecular Structure Center, Departments of Chemistry and Biochemistry, 100 West 18th Avenue, The Ohio State University, Columbus, OH 43210-1185, USA,* [b]*Ohio State Biochemistry Program, 100 West 18th Avenue, The Ohio State University, Columbus, OH 43210-1185, USA, and* [c]*Departments of Chemistry and Biochemistry, University of Washington, Seattle, WA 98195, USA. E-mail: sunda@biot.mps.ohio-state.edu*

(*Received 7 March 1997; accepted 22 September 1997*)

Abstract

The 1.89 Å resolution structure of the complex of bovine pancreatic phospholipase A_2 (PLA2) with the transition-state analogue L-1-*O*-octyl-2-heptylphosphonyl-*sn*-glycero-3-phosphoethanolamine (TSA) has been determined. The crystal of the complex is trigonal, space group $P3_121$, $a = b = 46.58$ and $c = 102.91$ Å and isomorphous to the native recombinant wild type (WT). The structure was refined to a final crystallographic R value of 18.0% including 957 protein atoms, 88 water molecules, one calcium ion and all 31 non-H atoms of the inhibitor at 1.89 Å resolution. In all, 7 726 reflections $[F>2\sigma(F)]$ were used between 8.0 and 1.89 Å resolution. The inhibitor is deeply locked into the active-site cleft and coordinates to the calcium ion by displacing the two water molecules in the calcium pentagonal bipyramid by the anionic O atoms of the phosphate and phosphonate group. The hydroxyl group of Tyr69 hydrogen bonds to the second anionic O atom of the phosphate group while that of the phosphonate group replaces the third water, 'catalytic' water, which forms a hydrogen bond to $N^{\delta 1}$ of His48. The fourth water which also shares $N^{\delta 1}$ of His48 is displaced by the steric hinderance of the inhibitor. The fifth conserved structural water is still present in the active site and forms a network of hydrogen bonds with the surrounding residues. The structure is compared with the other known TSA–PLA2 complexes.

1. Introduction

PLA2 is an extracellular calcium-dependent lipolytic enzyme that specifically cleaves the *sn*-2 ester bond of L-glycerophospholipid. The enzyme plays an important role in lipid metabolism and in interfacial catalysis. The family of PLA2 enzymes to which bovine pancreatic enzyme belongs shows a high degree of sequence homology and their overall three-dimensional structures are generally very similar. Calcium is an essential cofactor for substrate binding and catalysis. The enzyme has been implicated in a variety of physiologically important cellular processes such as inflammation and blood platelet aggregation. There is considerable interest in selecting potential inhibitors of the enzyme and to design suitable drugs to prevent chronic inflammation in rheumatoid arthritis.

Many crystal structures of the inhibitor TSA (Fig. 1*a*) complexed with PLA2 from different families are available. The TSA–inhibitor complexed with the extracellular PLA2 from Chinese cobra venom (White *et al.*, 1990) and human inflammatory exudate (Scott *et al.*, 1991) have been determined. A third

Table 1. *Crystal parameters and other relevant geometric parameters*

Cell dimensions (Å)	$a = b = 46.58$, $c = 102.91$
Resolution range (Å)	8.0–1.89
Crystal system, space group	Trigonal, $P3_121$
Measured reflections	44425
Unique reflections	8758
R_{sym} (%)	7.1
Cumulative completeness (%)	72 at 1.89 Å
R factor (%)	18.0
Protein model	
Protein atoms	957
Water molecules	88
Bound calcium ion (Ca^{2+})	1
Inhibitor atoms	31
R.m.s. deviation	
Bond lengths (Å)	0.014
Bond angles (°)	1.87
Parameter file	parhcsdx.pro
Topology file	tophcsdx.pro
Average atomic temperature factors of the refined model (Å^2)	
Main-chain atoms	17.7
Side-chain atoms	22.2
Calcium ion	11.2
Water molecules	32.8
Inhibitor atoms	30.3

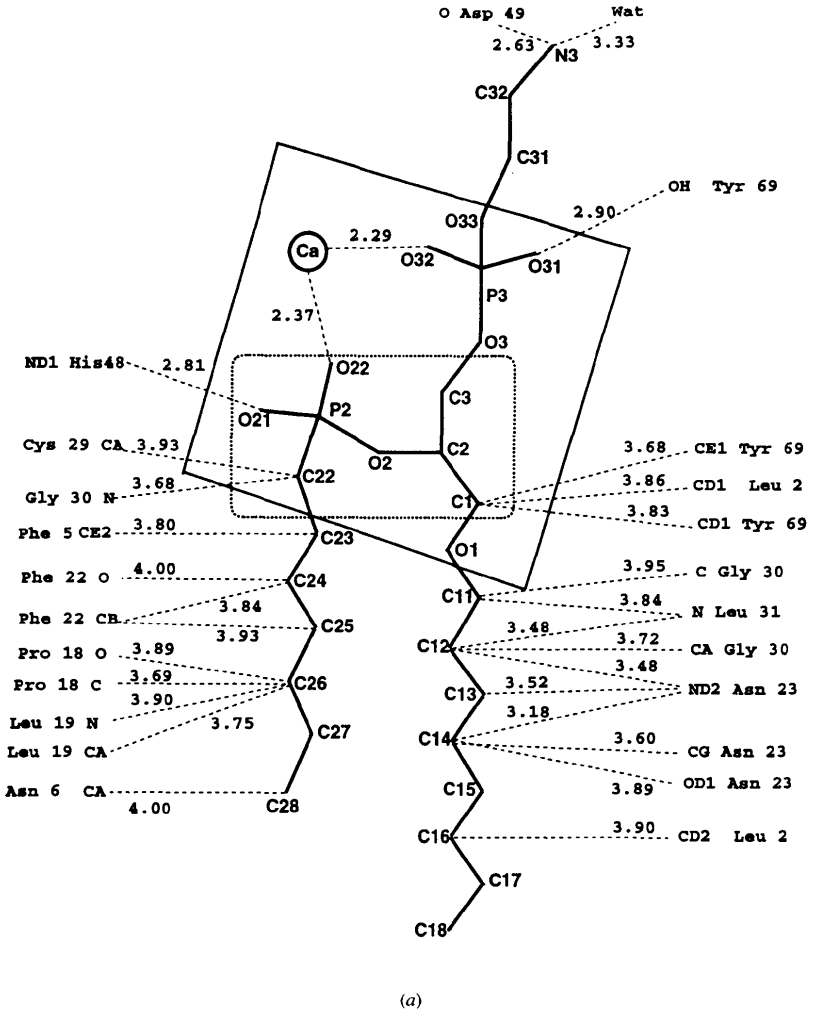

(*a*)

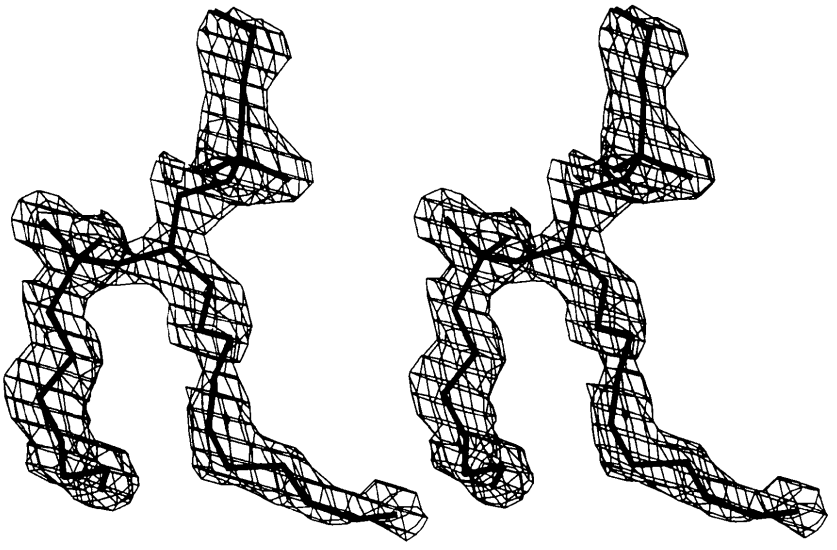

(*b*)

Fig. 1. (*a*) Schematic drawing of the transition state analogue inhibitor, L-1-*O*-octyl-2-heptylphosphonyl-*s*-*n*-glycero-3-phosphoethanolamine (TSA), and its distances (Å) to the conserved hydrophobic channel residues. The atoms within the solid box are not perturbed and are conformationally conserved for all the inhibitors. (*b*) A stereoview of the omit electron density of the inhibitor after the final refinement. Contours are shown at 1.0σ level.

complex of TSA–PLA2 has been determined from bee venom (Scott, Otwinowski *et al.*, 1990), although it is from a different family, the active-site structure is conserved with other PLA2's. However, TSA complexed with a pancreatic PLA2 has not been reported until this work. Other different non-TSA inhibitors complexed with PLA2 from porcine pancreas (Thunnissen *et al.*, 1990), bovine pancreas (Tomoo *et al.*, 1994) and human nonpancreatic PLA2 (Cha *et al.*, 1996) have also been determined. Here we report the crystal structure analysis of the TSA inhibitor complexed with the recombinant bovine pancreatic PLA2 and compare it with the other known TSA complexes.

2. Methods and materials

A crystal of the TSA inhibitor complexed with the recombinant bovine pancreatic PLA2 was obtained by co-crystallization by the hanging-drop vapor-diffusion method at room temperature (291 K). The crystallization droplet contained 5 µl protein solution 20 mg ml^{-1} in 50 m*M* Tris buffer, pH 7.2 and 2.5 µl of 2-methyl-2,4-pentane diol (MPD) (75%) and 2 µl of the

(*a*)

(*b*)

Fig. 2. A stereoview of the superposition of the Cα model of the present bovine pancreas PLA2 (thick lines) on (*a*) cobra venom PLA2 (dotted lines) and (*b*) inflammatory exudate PLA2 (thin lines). There are two molecules in the asymmetric unit of cobra venom and human inflammatory exudate, but only molecule *A* is shown. Side-chain atoms of the active-site residues are shown in thick lines. The active-site region superimposes very well.

inhibitor (2 m*M*) with the reservoir containing 50% MPD. After repeated trials these conditions yielded one good diffraction-quality crystal in three weeks. The crystal was trigonal, space group $P3_121$, with the unit-cell parameters $a = b = 46.58$ and $c = 102.91$ Å and isomorphous to the recombinant wild-type (WT) enzyme

The crystal of dimensions 0.2 × 0.2 × 0.3 mm was mounted in a glass capillary with mother liquid and sealed at both ends. X-ray intensity data were collected using our in-house Siemens area detector equipped with a four-axis goniostat and a Mac Science rotating anode which was operated at 50 kV and 90 mA at room temperature. The crystal-to-detector distance was 12.5 cm. The data were collected using two ω-scans and one φ-scan in 0.2° steps using a 60 s exposure time per frame. A total of 44 425 observations were measured which gave 8 758 unique reflections with an R_{sym} of 7.1%. The intensity data were reduced using the *XENGEN*2.0 software package (Howard, 1990).

The structure of the TSA inhibitor complex was solved by using the new atomic coordinates of the recombinant WT (Sekar *et al.*, 1998) as the starting model. Initial rigid-body refinement gave an *R* factor of

(*a*)

(*b*)

Fig. 3. (*a*) A stereoview of the recombinant bovine PLA2 enzyme showing the active-site cleft and the inhibitor TSA (ball and stick). Calcium ion is shown as grey circle and the disulfide bonds are shown. (*b*) The above view has been rotated (rotation −115° in *y* and −30° in *x*), which shows the atoms of the TSA inhibitor in the active site. Note the calcium-binding loop is above the inhibitor. The figures were produced using the program *MOLSCRIPT* (Kraulis, 1991).

27.8% for 7 726 reflections between 8.0 and 1.89 Å resolution for the protein atoms excluding the calcium ion and water molecules. The structure was refined using simulated-annealing techniques, from 3000 K and slowly cooling to 300 K, in steps of 25 K, using all the reflections in the range 8.0–1.89 Å to an R factor of 24.7%. The difference electron-density map revealed the position of the calcium ion and 50 water molecules and by including them, the R value dropped to 21.2% after positional and individual B-factor refinement for all the atoms. The inhibitor was fitted using $|F_o| - |F_c|$ and $2|F_o| - |F_c|$ difference electron-density maps and minor adjustments were made to the protein model by omit electron-density maps using the molecular modelling program *FRODO* (Jones, 1985). During the progress of the refinement additional water molecules

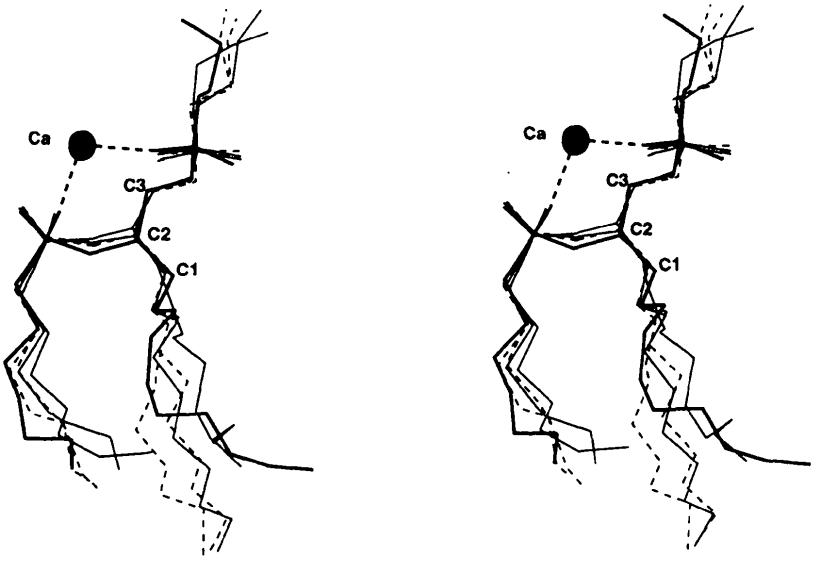

(*a*)

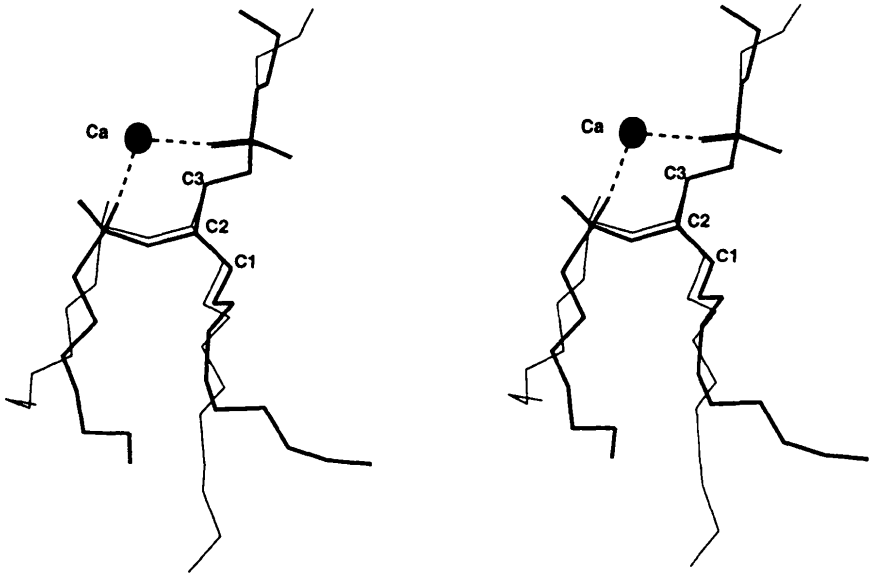

(*b*)

Fig. 4. (*a*) Superposition of the TSA inhibitor from bovine pancreas PLA2 (thick line) on that from cobra venom (two independent molecules, thin line) and human inflammatory exudate (two independent molecules, dotted line). (*b*) Superposition of the TSA inhibitor from bovine PLA2 (thick line) and bee venom PLA2 (thin line). Note the differences in the conformation of the last four atoms in both the *sn*-1-α and *sn*-2-β chains. The 14 atoms shown within the box (Fig. 1*a*) have been used for superposition. The calcium ion is shown as a filled circle.

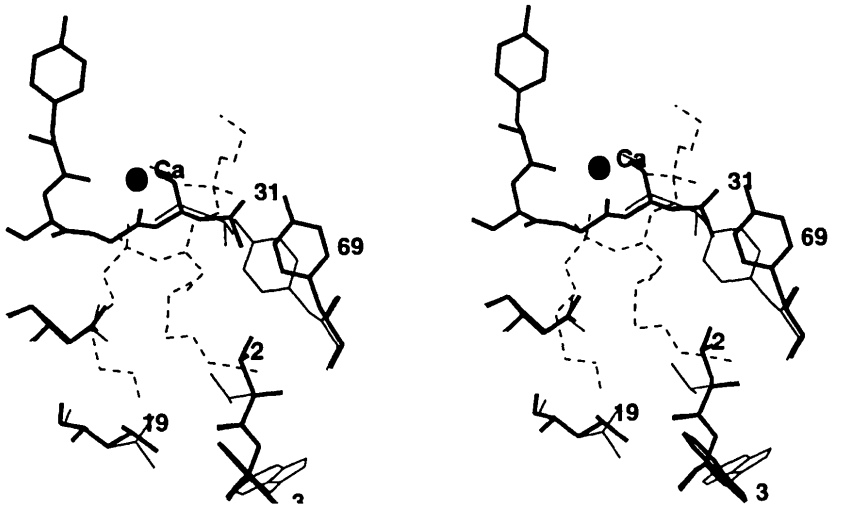

Fig. 5. A stereoview showing the superposition of the active-site region in the free PLA2 (thin lines) and the inhibitor complex (thick lines). The TSA inhibitor is shown in broken lines. Note the movements of many of the side chains (see text) in the inhibitor complex compared with the free PLA2.

were picked from the difference electron-density maps. In the final refinement cycles, a total of 88 water molecules were included. The R value dropped to 18.0% for 7 726 reflections [$F>2\sigma(F)$] between 8.0 and 1.89 Å for the entire TSA–PLA2 complex. All of the refinement calculations were carried out using *X-PLOR* version 3.1 (Brünger, 1992). The final protein model contains 957 non-H protein atoms (123 residues), 88 water molecules, 1 Ca^{2+} ion and all 31 atoms of the TSA inhibitor. The average B factors for the molecule are given in Table 1. The positional coordinate error is 0.2 Å (Luzzati, 1952). The quality of the protein model was assessed by *PROCHECK* (Laskowski *et al.*, 1993). All the (φ, ψ) values are in the allowed regions of the Ramachandran map. The atomic coordinates and the structure factors have been deposited with the Protein Data Bank.†

3. Results and discussion

The final refinement and selected geometrical parameters are given in Table 1. The protein model in the recombinant PLA2–inhibitor complex has been compared with the new atomic coordinates of the trigonal recombinant enzyme (Sekar *et al.*, 1998). A superposition of the main-chain Cα atoms gave a root-mean-square (r.m.s.) deviation of 0.24 Å, indicating that the overall tertiary fold is similar. The backbone Cα atoms of PLA2 from cobra venom (White *et al.*, 1990), inflammatory exudate (Scott *et al.*, 1991) and the present bovine pancreas PLA2 superimpose well within 0.87 Å (Fig. 2). All the 31 atoms of the TSA inhibitor could be readily fitted into the electron-density map (Fig. 1*b*). The temperature factor for the glycerol moiety (26.2 $Å^2$) (dotted box in Fig. 1*a*) is, as expected, lower than the terminal atoms of the fatty-acid chain (37.7 $Å^2$). The surface loop, residues 62–66 in the complex, is mobile and does not participate in binding to the inhibitor.

The TSA inhibitor is designed to emulate the tetrahedral transition state of the phospholipid substrate, where the phosphonate replaces the carboxyl *sn*-2 ester group (Yuan & Gelb, 1988). The binding of the inhibitor in the enzyme active-site cleft is shown in Fig. 3(*a*) and a rotated model with all the atoms of the TSA inhibitor resolved is shown in Fig. 3(*b*). The conformation of the TSA inhibitor in the bovine PLA2 complex is compared (Fig. 4) with the other known TSA inhibitors (Scott, Otwinowski *et al.*, 1990; White *et al.*, 1990; Scott *et al.*, 1991). The 14 atoms of the glycerol, the phosphate and the phosphonate moiety of the inhibitor (Fig. 1*a*) show only small variations of 0.15–0.52 Å upon superposition when compared with the TSA inhibitors in other PLA2 complexes. This similarity in the conformation of the glycerol moiety is probably because of the hydrogen bonding of the phosphate and phosphonate groups to the PLA2 enzyme. The fatty-acid chains adopt slightly different conformations which are magnified as one goes down the chain. In the TSA inhibitors, including the bovine complex, the *sn*-2-β-chain is similar in conformation but the last four atoms in bee venom are different (Fig. 4*b*). In the *sn*-1-α-chain the last four atoms are dissimilar in all the cases. The side chains of Leu2, Trp3, Leu19, Leu31 and particularly Tyr69 move considerably compared with the native enzyme in order to facilitate the entry and binding of the inhibitor in the active site

† Atomic coordinates and structure factors have been deposited with the Protein Data Bank, Brookhaven National Laboratory (Reference: 1MKV, R1MKVSF). Free copies may be obtained through The Managing Editor, International Union of Crystallography, 5 Abbey Square, Chester CH1 2HU, England (Reference: GR0739). At the request of the authors, the structure factors will remain privileged until 13 September 2001.

(Fig. 5). The Tyr69 hydroxyl group hydrogen bonds with an anionic O atom of the *sn*-3 phosphate and helps to anchor the inhibitor in the active-site cleft (Kuipers *et al.*, 1989). The inhibitor thus penetrates deep into the active site displacing the water molecules in the cleft and binds to the essential calcium ion by replacing the two coordinated water molecules and also the 'catalytic' water. The amino group of the ethanolamine head group of the inhibitor hydrogen bonds to the enzyme, backbone carbonyl group of Asp49, and a water molecule (Fig. 1*a*).

The calcium ion in the native enzyme has seven ligands arranged in a pentagonal bipyramidal geometry (Fig. 6*a*). Apparently the seven-coordinated calcium is required for PLA2 activity. In the present complex, as in other TSA–PLA2 complexes, the equatorial water W5 is replaced by the inhibitor phosphonate group and the axial water W12 by the phosphate group with hardly any perturbation of the calcium coordination geometry (Fig. 6*b*). The coordination of the inhibitor phosphonate O22 atom to calcium leads one to suspect that the *sn*-2 carbonyl O atom of the substrate also coordinates

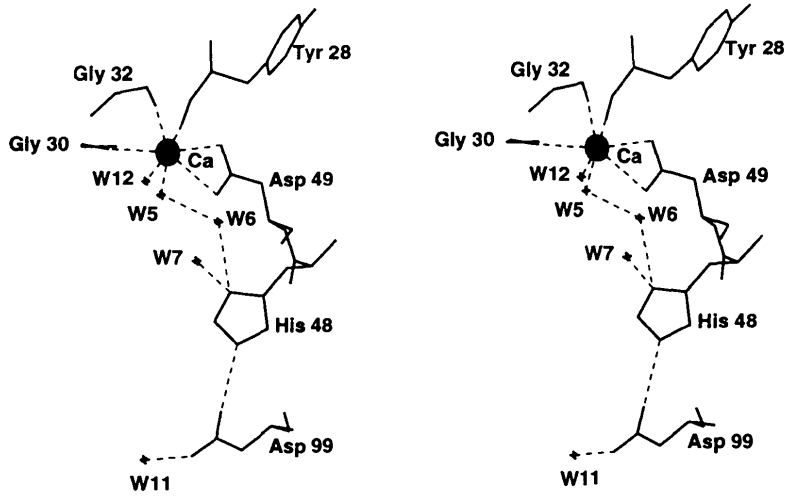

(*a*)

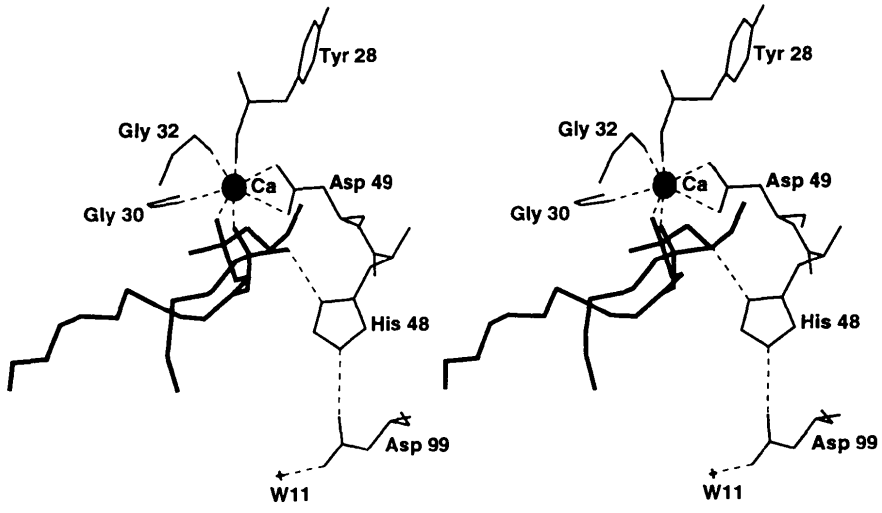

(*b*)

Fig. 6. (*a*) A stereoview of the free PLA2 structure showing the two water molecules (W5 and W12) in the calcium coordination, the structural water (W11) and the two waters (W6 and W7) hydrogen bonded to Nδ1 and lying on either side of the imidazole plane of His48. (*b*) Stereoview of the TSA complex showing that the water molecules (W5, W6 and W12) are replaced by the inhibitor phosphate/phosphonate anionic O atoms while W7 is dislodged by the close approach of the C3 atom of the inhibitor. The structural water is retained in the present PLA2–TSA complex.

to the calcium ion to delocalize its electrons and facilitate the nucleophilic attack by the water to form the tetrahedral intermediate (Scott, White *et al.*, 1990).

The catalytic water, W6, and the extra water W7, lie above and below the imidazole ring of His48 and share $N^{\delta 1}$ in hydrogen bonding (Fig. 6*a*). In the complex, the catalytic water is replaced by the anionic O21 atom of the inhibitor phosphonate group while W7 (Fig. 6*a*) is removed by the steric bulk of the inhibitor C3 atom (Fig. 6*b*). Similar short contacts are observed in the other PLA2–TSA complexes. The conserved structural water W11 (Fig. 6*b*) in the enzyme complex is present because it is far away (8.87 Å) from the inhibitor. This water forms a network of hydrogen bonding with the surrounding active-site residue Asp99, the interfacial site residues Ala1, Tyr52, Tyr73 and the carbonyl O atom of Pro68 as in the native structure. The inhibitor also displaces three water molecules in the active-site pocket.

This work was supported by National Institutes of Health (NIH) research grants GM 45947 to MS, GM41788 to MDT and HL 36235 to MHG and an Ohio Regents Eminent Scholar Chair to MS.

References

Brünger, A. T. (1992). *X-PLOR* Version 3.1. *A system for X-ray crystallography and NMR*. New Haven, Connecticut, USA.

Cha, S.-S., Lee, D., Adams, J., Kurdyla, J. T., Jones, C. S., Marshall, L. A., Bolognese, B., Abdel-Meguid, S. S. & Oh, B.-H. (1996). *J. Med. Chem.* **30**, 3878–3881.

Dijkstra, B. W., Drenth, J. & Kalk, K. H. (1981). *Nature (London)*, **289**, 604–606.

Howard, A. J. (1990). *A guide to macromolecular X-ray data reduction for the Siemens area detector system. The XENGEN system, version* 2.0, Genex Corporation, Gaithersburg, Maryland, USA.

Jones, T. A. (1985). *Methods Enzymol.* **115**, 157–171.

Kraulis, P. J. (1991). *J. Appl. Cryst.* **24**, 946–950.

Kuipers, O. P., Dijkman, R., Pals, C. E., Verheij, H. M. & de Haas, G. H. (1989). *Protein Eng.* **2**, 467–471.

Laskowski, R. A., MacArthur, M. W., Moss, D. S. & Thornton, J. M. (1993). *J. Appl. Cryst.* **26**, 283–291.

Luzzati, V. (1952). *Acta Cryst.* **5**, 802–807.

Noel, J. P., Bingman, C. A., Deng, T., Dupureur, C. M., Hamilton, K. J., Jiang, R. T., Kwak, J. G., Sekharudu, C., Sundaralingam, M. & Tsai, M.-D. (1991). *Biochemistry*, **30**, 11801-11811.

Scott, D. L., Otwinowski, Z., Gelb, M. H. & Sigler, P. B. (1990). *Science*, **250**, 1563–1566.

Scott, D. L., White, S. P., Browning, J. L., Rosa, J. J., Gelb, M. H. & Sigler, P. B. (1991). *Science*, **254**, 1007–1010.

Scott, D. L., White, S. P., Otwinowski, Z., Yuan, W., Gelb, M. H. & Sigler, P. B. (1990). *Science*, **250**, 1541–1546.

Sekar, K., Sekharudu, C., Tsai, M.-D. & Sundaralingam, M. (1998). *Acta Cryst.* D**54**, 342–346.

Thunnissen, M. M. G. M., Eiso, A. B., Kalk, K. H., Drenth, J., Dijkstra, B. W., Kuipers, O. P., Dijkman, R., de Hass, G. H. & Verheij, H. M. (1990). *Nature (London)*, **347**, 689–691.

Tomoo, K., Ohishi, H., Ishida, T., Inoue, M., Ikeda, K., Sumiya, S. & Kitamura, K. (1994). *Proteins*, **19**, 330–339.

White, S. P., Scott, D. L., Otwinowski, Z., Gelb, M. H. & Sigler, P. B. (1990). *Science*, **250**, 1560–1563.

Yuan, W. & Gelb, M. H. (1988). *J. Am. Chem. Soc.* **110**, 2665–2666.